

# Influence of Beam Polarization on Laser Cutting Efficiency

V.G.Niziev, A.V.Nesterov

NICTL-Laser Research Center of Russian Academy of Sciences  
Shatura 140700, Russia

**ABSTRACT.** The 3D theory of laser cutting is presented. The cutting efficiency determined by its ultimate parameters at different types of polarization is estimated. It is shown that ultimate cutting characteristics at plane P-polarized beam are essentially worse in comparison with potential possibilities connected with P-wave absorption. The physical reasons for this limitation are illustrated. For cutting metals with a large ratio of sheet thickness to width of the cut laser cutting efficiency for radially polarized beam is 1.5-2 times more than for plane P-polarized and circularly polarized beams. The possibility of the radially polarized beam generation is discussed.

## 1. INTRODUCTION

Laser cutting of metals is one of the most widespread methods of laser processing. The practice of laser cutting poses a number of basic problems. One of the most important problems is increasing laser cutting efficiency. Laser cutting efficiency, defined as a ratio between energy expenses for material removal and input energy, is about 20% and efficiency of the laser itself is less than 20%. To date there exist two directions in laser cutting of metals: cutting thin sheets with a small ratio of thickness ( $h$ ) to cutting width ( $d$ ) and thick sheets, for which  $h/d \geq 10$ . For cutting thin metal sheets they use lasers of comparatively low output power, generated in the  $TEM_{00}$  mode. The sharp focusing of radiation is necessary for high-speed cutting of thin sheet steel. Frequently they use plane polarized radiation with maximal absorption at the cut front, in comparison with the absorption on the walls. In this case such a polarization has certain advantages.

With laser cutting of thick metal sheets, the situation is different. On the one hand, lenses of longer focal length are used, therefore the advantage of the main mode appears less essential. On the other hand, the use of the main mode in lasers of higher power is a difficult task to be solved. Therefore, lasers of different transverse mode structure ( $TEM_{00/01*}$ ,  $TEM_{01*}$ ) are used.

In the case of  $h/d \geq 10$  the question of optimum polarization remains open until the present time. Yet in the early study [1] the basic features of laser cutting with plane-polarized radiation were investigated theoretically and experimentally. It was noted that the maximum efficiency of laser cutting with plane-polarized radiation is achieved when most energy is absorbed in the front of the cut, i.e. cutting direction is parallel to the oscillation plane of the electric field vector. But even then

many firms produced industrial lasers with the circular polarization. This tendency remains up to now. The up-to-date technological systems for metal cutting use circularly polarized radiation, although the plane P-polarized beam with maximum absorption on the cut front seems to be the best for this application.

As for theoretical investigations, a great deal of them involves the particular aspects of laser cutting such as heat diffusion at moving heat source, hydrodynamic processes, the role of oxygen, formation of striations on the cut walls, and so on [2-7]. These authors used the simplified concepts of radiation absorption and the cut shape.

In some studies, radiation absorption was considered in accordance with Fresnel laws. For example, cutting with a P-polarized laser beam at the cut front was treated in [8]. The recommendations were given for focus position and mode structure, but the influence of different polarization types on cutting parameters was not analyzed.

The ultimate cutting depth was calculated by the use of the 3D metal cutting model [9]. The authors used the following restrictions in calculations: energy density over the beam cross-section was constant and peculiarities of absorption on the cut walls were not taken into account.

Another 3D laser cutting model [10] is also noteworthy. The authors considered the influence of different parameters (intensity, polarization, focus position, mode structure, laser beam divergence) on cutting processes. The fundamental restriction of this consideration was a simplified description of the cut shape that was not calculated. Such an approach excludes the possibility of analyzing the cause of restrictions on ultimate cutting parameters.

In paper [11] the 2D laser cutting task taking into account the intensity distribution according to Gauss law and Fresnel absorption on the cut front, was solved. The front shape was found from the stationary solution at different types of polarization and focus positions in the co-ordinate system connected with the beam. The solution for fluctuations determined the instabilities development area on the cut front, the velocity of fluctuation movement, along the front and the increment of their development.

## **2. MATHEMATICAL MODEL**

The problem of 3D cut shape description has been solved in the present study. This description takes into account radiation absorption on the whole cut surface: both on the front and on the walls. This approach allows comparisons of the efficiency of the action of different laser beam polarization (plane, circular, and so on) on material from the same viewpoint.

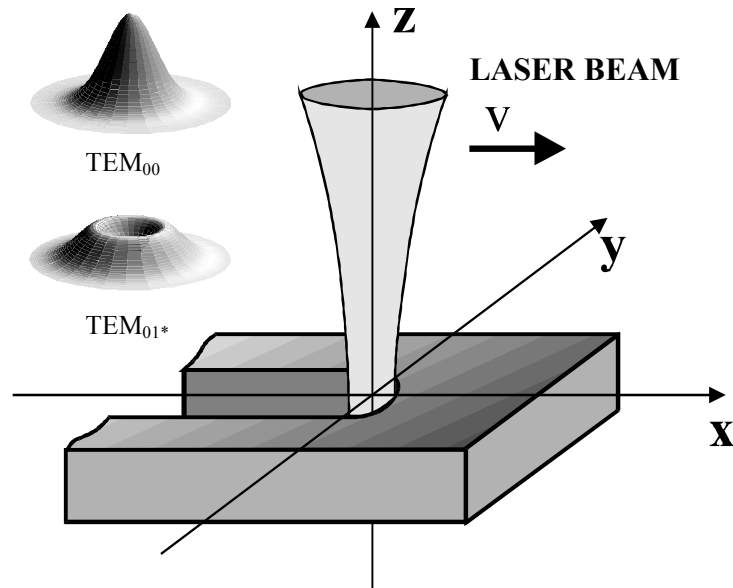


Fig. 1. The scheme of sample and laser beam positions in the used coordinate system.

Laser cutting of metal is carried out with gas jet directed at high pressure into the kerf. The main function of gas jet is the removal of the melted material. The hydrodynamic processes are very fast under current conditions of intense gas jet use. So the material is considered to be removed instantly. Thus a detailed description of hydrodynamic processes becomes unnecessary.

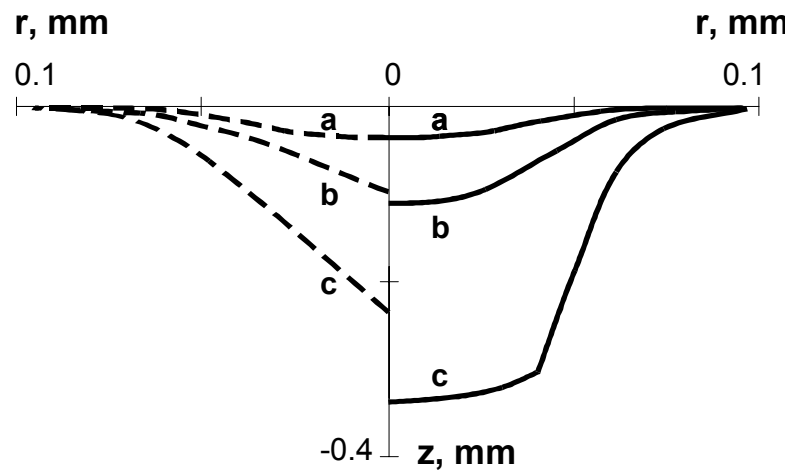


Fig. 2. Laser beam hole punching. Evolution of depth and form at azimuthal (left) and radial (right) polarization (A and R, Table 1). The curves a, b, c correspond to the time moments  $t_1 < t_2 < t_3$ .

The chemical reactions on the cut surface are not discussed in the present paper. This relates directly to laser cutting without oxygen. The problem of effective and qualitative metal cutting without oxygen is real [12]. The aspects of radiation absorption with different polarization types discussed in the present study are also important for cutting with oxygen.

In real cutting conditions, the main portion of heat is concentrated in the melted material removed from the kerf with gas flow. The temperature distribution is localized in the thin surface layer. Therefore heat conduction processes are neglected in the present model.

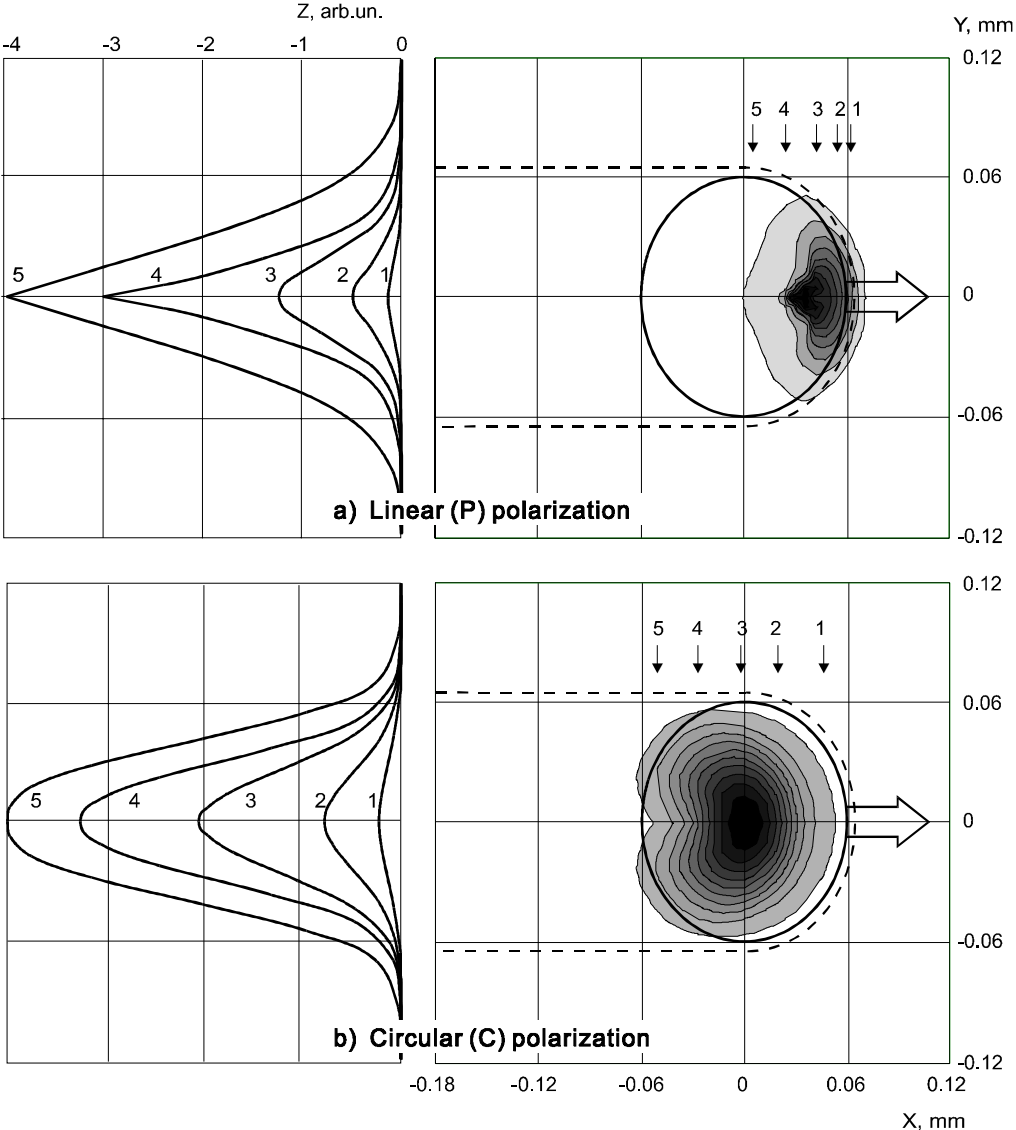


Fig. 3. Cut form projection on y-z-plane (left) and the distribution of absorbed laser power over the cross section of the laser beam (right) for plane (P) and circular (C) polarization. Absorbed laser power is equal to  $I \times F$ , see (3). The circle shows the border of a laser beam schematically, the large arrow is the direction of beam movement, the dotted line is cut contours.

The model is being considered within the limits of geometrical optics approximation. Only single reflections have been taken into account. The cut has an open shape in comparison with the channel at laser beam hole punching. Radiation, reflected from the laser beam action area, is scattered on the cut walls outside this area. Thus the reflected radiation does not contribute to material destruction and dissipates in metal by thermal conductivity.

The aspect ratio of laser cutting (the ratio of the depth to the width) is about 10 in practice. It means that the main part of the radiation interacts with material at large angles close to the main

angle ( $\sim 85^\circ$  for steel). In our model we used the classical Fresnel formulae for metals with complex index of refraction. A significant feature of this absorption law is the sharp dependence of P-wave absorption on large angles of incidence. Such behavior of the absorption coefficient is retained, when the surface temperature rises. So taking into account the dependence of absorption on temperature would not lead to qualitative changes at high temperatures up to  $3000^\circ\text{K}$  and can only give some quantitative specification [13].

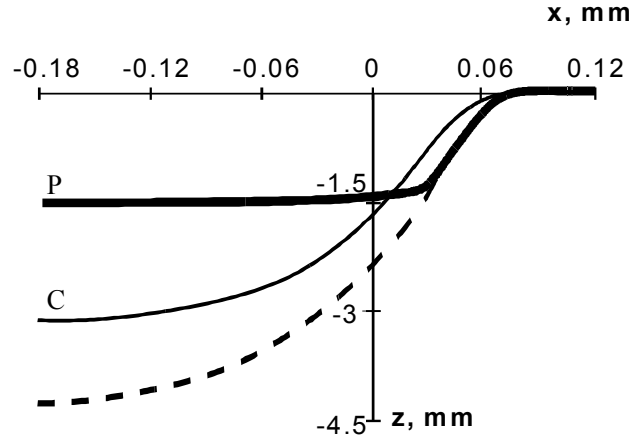


Fig. 4. Cut profiles in x-z-plane at  $y=0$  for P- and C-types of polarization. Laser mode  $\text{TEM}_{00}$ . The dotted line is a potential channel profile without taking into account absorption on the walls.

The scheme of sample and laser beam relative positions in the used coordinate system is presented in Figure 1. The intensity of the beam moving along x-axis with the velocity  $v$  is

$$I(x, y, z, t) = \frac{I_0}{1 + L(z)^2} \exp\left[-\frac{2((x - vt)^2 + y^2)}{r_0^2(1 + L(z)^2)}\right], \quad (1)$$

where  $L(z) = \frac{z - z_f}{z_0}$ ,  $z_0 = \pi r_0^2 / \lambda$ ,  $r_0$  is the laser beam spot radius and  $z_f$  is the laser beam focus position in relation to the sample surface.

In all the further expressions  $z$  is a calculated function of independent arguments  $x$ ,  $y$ ,  $t$ . Local energy balance in a point on the cut surface has the form:

$$V_n = k P, \quad (2)$$

where  $V_n$  is the material removal velocity in normal direction to the surface and  $\mathcal{D}$  is the density of absorption power, which is defined as

$$P = I(x, y, z, t) F(\alpha, \beta - \beta_0) \cos(\alpha) \quad . \quad (3)$$

Here  $F(\alpha, \beta - \beta_0)$  is the absorption coefficient,  $\alpha$  is the angle of the laser beam incidence on the surface ( $\alpha = \arctg \sqrt{z_x^2 + z_y^2}$ ),  $\beta$  is the angle between the incidence plane of the laser beam and its movement direction ( $\beta = \arctg(z_y / z_x)$ ). In the case of a plane polarized beam, the angle  $\beta_0$  between the electric field vector and the vector of beam velocity is constant.

For a plane polarized beam  $F(\alpha, \beta - \beta_0)$  is given by the formula

$$F_L(\alpha, \beta - \beta_0) = F_S(\alpha) \sin^2(\beta - \beta_0) + F_P(\alpha) \cos^2(\beta - \beta_0), \quad (4)$$

where  $F_S(\alpha)$ ,  $F_P(\alpha)$  are Fresnel formulae for S- and P- wave absorption. In the case of circular polarization the absorption coefficient depends only on  $\alpha$ :

$$F_C(\alpha) = (F_S(\alpha) + F_P(\alpha)) / 2. \quad (5)$$

Coefficient  $k$  in (2) depends on thermal properties of the material and is a constant value. By removal of the melted material with gas flow,  $k$  is given by:

$$k = (c\rho(T_1 - T_0) + \mu)^{-1}, \quad (6)$$

where  $\tilde{n}$ ,  $\rho$ ,  $\mu$  are specific heat, density and melting heat of the material;  $T_0$ ,  $T_1$  are the initial temperature and the melting temperature of the material.

Because of the threshold character of material destruction, formula (2) is valid only for high densities of absorbed power  $P$ , which exceed the threshold value. Such conditions must exist in the beam action area where the main radiation power is contained. In particular, the use of the present model is restricted at low beam velocity  $v$ . If the focus was on the sample surface and  $v$  was low, the radiation intensity could decrease at high channel depth in such a way that the absorbed power density would be below the threshold of destruction. The approximation determined by equation (2) is fully justified for the wide spectrum of laser cutting parameters.

The equation of surface kinematic compatibility is

$$dN/dt = 0, \quad (7)$$

where  $N = z - z(x, y, t)$ . Formulae (2) and (7) form an equation system that is transformed into a nonlinear partial equation by  $x, y, t$  written in the co-ordinate system connected with the laser beam:

$$\partial z / \partial t = v \partial z / \partial x - kI(x, y, z) F(\alpha, \beta - \beta_0). \quad (8)$$

By analogy [11], the stationary part  $z_s(x,y)$  of the general solution  $z(x,y,t)=z_s(x,y)+\delta(x,y,t)$  is calculated from

$$v \partial z_s / \partial x = kI(x,y, z_s) F(\alpha, \beta - \beta_0). \quad (9)$$

The stationary solution  $z_s(x,y)$  defined by equation (9) exactly describes the surface under a stable cutting regime. In real laser processing conditions convective instabilities with low amplitude develop on the cut surface [14]. One can speak about their movement along the surface  $z_s$ . Increasing instability amplitude is restricted by time, during which the instabilities move in the beam action area.

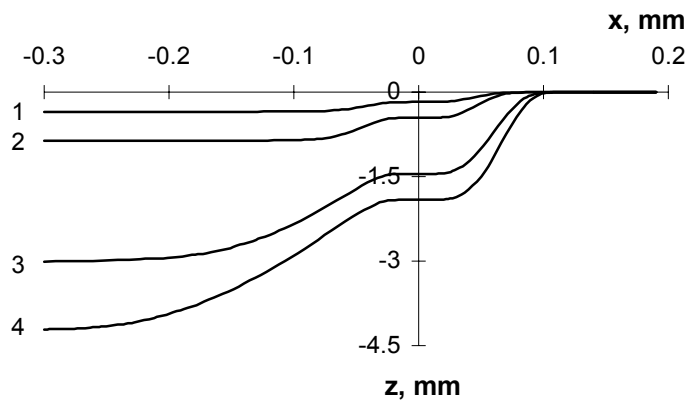


Fig. 5. Cut profiles in x-z-plane at  $y=0$  for C-polarization (curves 1, 3) and R-polarization (curves 2, 4). Ratio of beam intensity to velocity  $I_0/v$  for curves 3, 4 is ten times larger than for curves 1, 2. Focus is on the sample surface. Laser mode  $TEM_{01}^*$ .

Taking into account the instabilities of the front can change the calculated results only if we assume that the developing instabilities change the nature of absorption significantly and the classical Fresnel formulae are not acceptable. At the present time, there is no common opinion about the physical nature of these instabilities. No reliable data on their influence on the absorption coefficient are available. Meanwhile, the polarization of the radiation affects the parameters of the cut according to the S- or P-wave absorption. This universally recognized fact is indirect evidence of the immaterial role of the front instabilities in the absorption process.

The parameters of the model are: coefficient  $\hat{A}=kI_0/v$ , beam parameters  $r_0$  and  $z_0$ , components of complex refractive index of metal  $n(1+im)$  and focus position  $z_f$ .

Equation (9) has been solved by the method of characteristics. Calculation of each of the specific characteristics starts from a point on the semi-circumference having its center on the beam axis and radius  $R \gg r_0$  on the sample surface:

$$x^2 + y^2 = R^2; \quad x > 0.$$

The following expressions are valid along the semi-circumference:

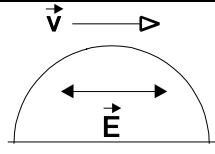
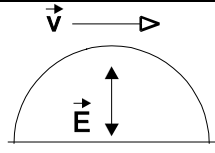
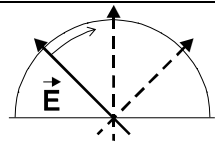
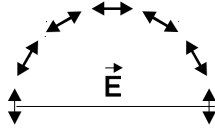
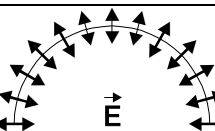
$$z'_x = k \cdot I(x, y, 0) \cdot F(z'_x, z'_y)$$

$$z'_x \cdot dx + z'_y \cdot dy = 0$$

Passing through the beam action area, the characteristics form the cut surface.

Within the framework of the present mathematical model the cut shape is described from the sample upper surface to the ultimate depth of material removal. When the sample thickness is less than the ultimate depth, the part of the solution that exceeds the sample thickness may not be taken into account. The list of laser beam polarization types on which the calculations have been carried out is given in Table 1.

Table 1. Types of laser beam polarization used for calculation.

Laser beam polarization type	Schematic view	Designation in the text
Plane polarization, an electrical vector is parallel to the beam velocity vector	 <p>The diagram shows a semi-circle with a horizontal diameter. A horizontal arrow labeled <math>\vec{v}</math> points to the right above the semi-circle. Inside the semi-circle, a horizontal double-headed arrow labeled <math>\vec{E}</math> is centered along the diameter.</p>	P
Plane polarization, an electrical vector is perpendicular to the beam velocity vector	 <p>The diagram shows a semi-circle with a horizontal diameter. A horizontal arrow labeled <math>\vec{v}</math> points to the right above the semi-circle. Inside the semi-circle, a vertical double-headed arrow labeled <math>\vec{E}</math> is centered along the diameter.</p>	S
Circular polarization	 <p>The diagram shows a semi-circle with a horizontal diameter. A dashed vertical line passes through the center. A solid line with an arrowhead at the top-left end is drawn from the center to the arc. A double-headed arrow labeled <math>\vec{E}</math> is drawn along this solid line.</p>	C
Azimuthal polarization	 <p>The diagram shows a semi-circle with a horizontal diameter. A double-headed arrow labeled <math>\vec{E}</math> is centered along the diameter. Multiple small double-headed arrows are drawn along the arc, all pointing in the same direction (upwards).</p>	A
Radial polarization	 <p>The diagram shows a semi-circle with a horizontal diameter. A double-headed arrow labeled <math>\vec{E}</math> is centered along the diameter. Multiple small double-headed arrows are drawn along the arc, all pointing radially outwards from the center of the semi-circle.</p>	R



### 3. RESULTS AND DISCUSSION

It was taken in all the calculations that  $\lambda=10.6 \mu\text{m}$  and  $r_0=0.06 \text{ mm}$ . The calculations were carried out for steel ( $m=3$ ,  $n=4.2$ ).

The special feature of the calculation results was the presence of two qualitative different shapes of cut surface depending on the law of radiation absorption on channel walls. The first shape conforms to the classical solution of equation (9). It is smooth and offers continuous first-order derivatives. The second one is a non-classical one with discontinued first-order derivatives, which leads to a break on the cut surface.

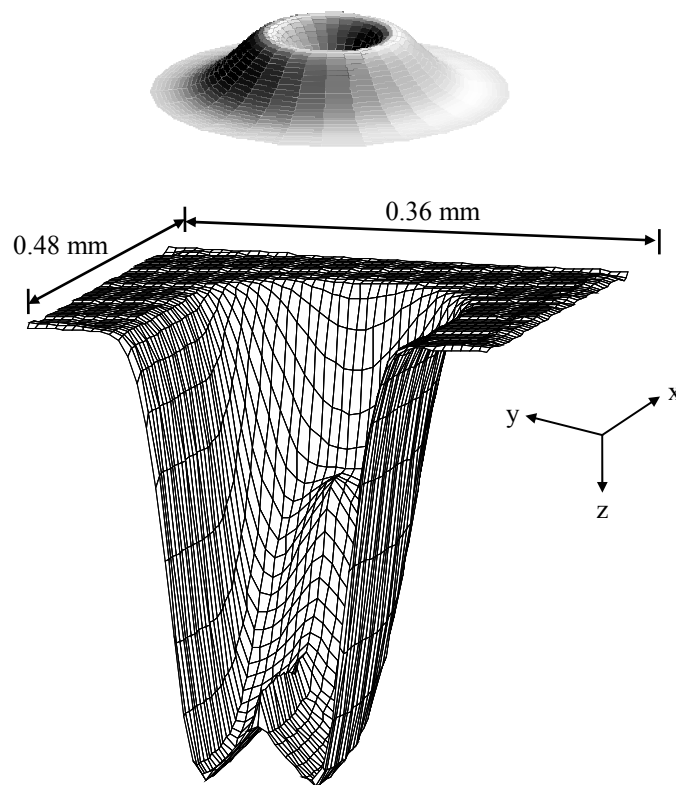


Fig. 6. Computed cut shape at the steel cutting with laser mode TEM01\*. Radial polarization. Focus is on the sample surface.

First let us consider the physical causes of such solutions for the case of laser beam punching. This problem was considered in [15,16]. The results for laser beam punching with A- and R-polarized beams are presented in Figure 2. By analogy [15], the cavity shape in the case of A-polarized beam corresponds to the classical solution with continuous first derivatives and is smooth at the beginning (Fig. 2a). The maximum absorption power density lays in the channel center: radiation intensity  $\sim I_0$ , the angle of incidence  $\alpha=0$  (for the smooth shape at short times). The break of the shape takes place at some certain depth at the critical point. Having appeared at this point, the angle between the walls decreases with time. The angle of incidence and therefore the absorption coefficient decrease, the energy input used for material removal is reduced. The potential

possibilities connected with the channel depth in the center by  $\alpha=0$  are not realized in this case. The real depth is lower than it could be for the smooth shape with the flat bottom. Thus, one can speak about the self-organization effect, which occurs in shape evolution to minimum radiation absorption.

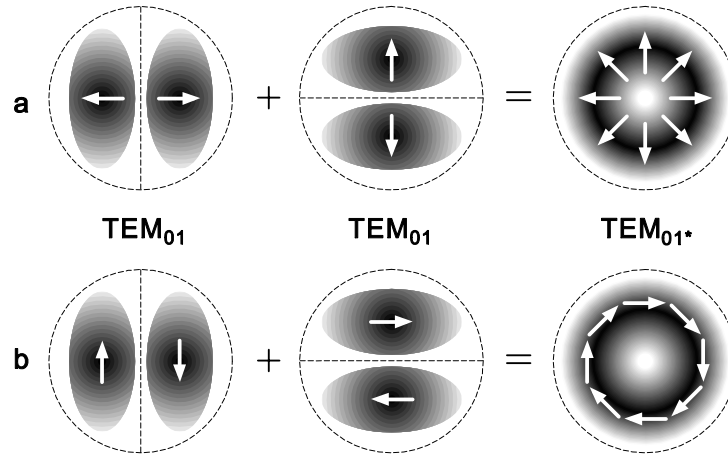


Fig. 7. Formation of  $TEM_{01*}$  mode with radial (a) and azimuthal (b) polarization as superposition of two plane polarized modes  $TEM_{01}$  [18].

In the case of R-polarized beam, the maximum density of absorption power is not at the bottom, but on the walls. So the break of the channel shape occurs on the walls, not at the bottom. The channel shape evolves eventually to the vertical walls and the flat bottom. The considered peculiarities of shape formation by laser beam punching bear a direct relation to laser cutting, thus restricting the efficiency of this process in certain cases.

In the cases of metal laser cutting by polarized beam (P, S, C, A, R, Table 1), the channel shape can in principle have breaks of the first derivative, which correspond to the non-classical solution of equation (9). These breaks can appear in the plane of channel symmetry ( $y=0$ ) in the case of P- and A- polarized beams or on the walls in the other cases (S, C, R).

We will not discuss the action of S- and A-polarized radiation in detail. The coefficient of absorption at the cut front is low for these types of polarization. The cutting parameters are correspondingly low. Therefore these cases have no practical importance.

The effect of channel shape breaking manifests itself most strikingly in the case of P-polarized beam over a wide value spectrum of coefficient B. This fact corresponds to the specific channel shape with an acute angle between the walls at the bottom, Figure 3a. The break introduces alterations to the absorption law for this surface. If the channel shape was smooth, material removal in the section  $y=0$  would be determined by P-wave absorption. In the case of V-shape (Figure 3a), the region with such P-wave absorption in the field of maximum intensity around the beam axis disappears. Absorption decreases on the cut surface because now the portion of S-wave prevails.

The ultimate cutting parameters become lower in comparison with the expected ones. Such a phenomenon can be interpreted as “sticking” of the laser beam in the material between the badly destroying channel walls. In the case presented in Figure 3a the V-shape of the channel is formed quite fast (curve 4), so in the centre of the laser beam, the absorbed power is very low although the intensity of radiation is maximum here. The absorption region is located in a small part of the laser beam cross section. Naturally only this part of the beam forms the cut front. The smaller the parameter B (it is determined in the text following (9)) taken for calculations, the bigger the absorption area will be. So such a limitation on laser power absorption is more for the laser cutting of thick metal sheet with big  $h/d$ .

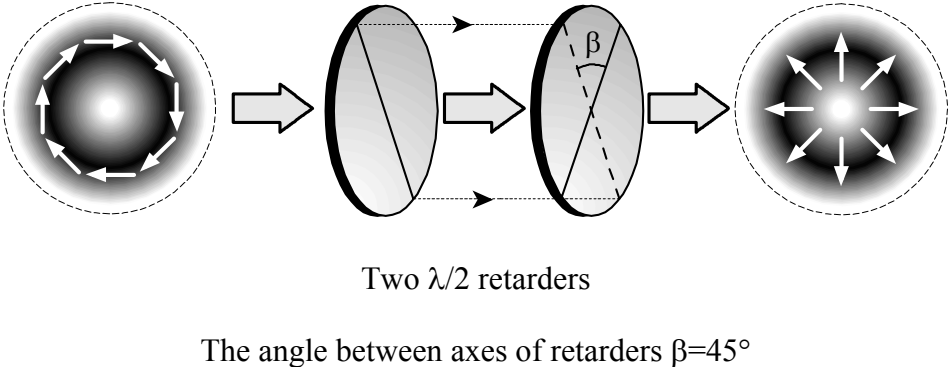


Fig. 8. The scheme of transformation of the beam with the azimuthal polarization to the beam with the radial polarization.

That is why the ultimate cutting parameters for the P-polarized beam in comparison with the S-polarized beam differ only 1.5-2 times [17], while the P-wave absorption coefficient is many factors of tens higher in comparison with the S-wave absorption coefficient at the main angle.

In the case of C-polarized beam, the break of the channel surface can occur on the channel walls. The region with maximum radiation absorption disappears at the angles of incidence close to the main angle. This kind of break has less consequences if compared with the case of P-polarized beam. The most important factor is that the beam does not “stick” in the plane of channel symmetry. The material is removed from the front and from the walls in such a way that the cut shape does not prevent the beam penetrating into the material (Figure 3b). The absorption region has approximately the same form as the laser power distribution region. The cut front is formed along the diameter of a laser beam. Such a picture remains the same at the different values of parameter B.

The calculated cut profiles in x-z-plane for the P- and C-polarized beams are shown in Fig. 4. The potential cutting depth for P-polarization calculated according to radiation absorption on the front is shown by the dotted line. The real profile (line P) coincides with the dotted line only in the beginning, at small z. The difference between the ultimate depth for the dotted line and line P is due

to the surface evolution to the shape with minimum radiation absorption (Fig. 3a). In the case of C-polarized beam, the front is more gentle and the ultimate cutting depth is larger. The ratio of ultimate depth for P- and C-types of polarization can be different and depends on the slope angle of the front and walls at specified cutting parameters. In any case the ultimate cutting parameters for the C-polarized beam turn out not worse than for the P-polarized beam [17].

As for the laser cutting efficiency and the ultimate cutting parameters, the axis symmetrical structure of polarization is preferable to plane P-polarization and especially to plane S-polarization. This is so in spite of the absorption coefficient on the cut front for C-polarization which is an average value of P- and S-wave absorption.

The preceding calculations were carried out for the laser  $TEM_{00}$  mode. The comparison of cutting parameters for the R- and C-polarized beams were conducted for the laser  $TEM_{01*}$  mode (Fig. 5). The better cutting parameters for the R-polarized beam are easily explicable. The coefficient of absorption is determined by P-wave absorption in the case of the R-polarized beam and by the arithmetical mean of P- and S-wave absorption in the case of the C-polarized beam. The ratio of ultimate depths for both the polarization types depends on parameter B, i.e., on material properties, radiation power and beam velocity. Maximum gain owing to the advantages of material processing with the R-polarized beam consists of increasing depth or cutting speed by 1.5-2 times in comparison with the C-polarized beam. The presence of “shelf” on the curves (Fig..5, 6) at  $x \sim 0$  is due to the ring structure of intensity distribution in laser mode  $TEM_{01*}$ .

Radial polarized radiation can be obtained on the basis of the laser  $TEM_{01*}$  mode [18]. The laser  $TEM_{01*}$  mode is a superposition of two laser  $TEM_{01}$  modes turned around the beam axis by  $90^\circ$  relative to each other. This «doughnut» mode is circular in cross section but hollow in the centre [19]. The resonators of the modern technological lasers commonly contain the element that provides for the plane polarization in all the transverse modes. The radial polarized  $TEM_{01*}$  can be obtained only when both the laser  $TEM_{01}$  modes have mutually perpendicular polarization (Fig. 7a). The generation of azimuthal polarization of the  $TEM_{01*}$  mode is shown in Fig. 7b.

Hence, the stable radial polarization of mode  $TEM_{01*}$  requires the specific polarization and the appropriate phase oscillation in the  $TEM_{01}$  modes. The technical solutions to this problem seem to be quite real. One of them uses a total mirror of conical form, which produces a beam with azimuthal polarization. Azimuthal polarization can be transformed to radial polarization by means of optical elements outside the resonator (Fig. 8). Here two phase reflecting retarders  $\lambda/2$  are turned in such a way that the angle between their axes is  $45^\circ$ . Then the output radiation acquires radial polarization. There are also some possibilities to transform circular polarization into radial polarization outside the resonator.

#### 4. CONCLUSION

The absorption of radiation on the cutting surface is the main physical process, which determines the cutting parameters. To adequately describe this process, the 3D problem of the cut calculation has been solved. Within the framework of this problem the ultimate laser cutting parameters have been estimated. A comparison of cutting efficiency for different polarization types and mode structures has been carried out.

The significant peculiarity of the calculation results is the presence of two qualitative different shapes of cut surface depending on the law of radiation absorption on channel walls. The first shape is smooth and offers continuous first-order derivatives. The second has discontinued first-order derivatives, i.e., breaks on the cut surface.

The P-polarized beam forms the shape with the break at the bottom. This V-shape results from low radiation absorption on the cut walls. It restricts the ultimate cut depth as the area with prevailing P-wave absorption disappears.

Such a restriction does not hold for axis-symmetrical polarization types (C, R). In these cases the breaks of the shape can appear on the walls but not at the bottom. They do not impede the beam penetrating into the material. The action of R- and C-polarized beams is characterized by P-wave absorption and by the arithmetic mean of S-wave and P-wave absorption on the whole cutting surface correspondingly. Therefore the ultimate depth and cutting speed for R-polarization are 1.5-2 times higher than the same parameters for C-polarization.

According to the calculations, C-polarized radiation is preferable to plane polarized radiation at the  $TEM_{00}$  mode. R-polarized radiation is the most effective for cutting with the laser  $TEM_{01*}$  mode.

The physical reason for restrictions on laser cutting depth at L-polarization considered in this paper is connected to the large difference in absorption on the front and on the walls. This takes place at the large  $h/d$  ratio, when the angle of incidence is close to the main angle. For cutting thin metal sheets with the small  $h/d$  ratio the increased absorption on the front in comparison with absorption on the walls is insignificant, and the considered restrictions on the use of the D-polarized radiation also become insignificant.

One of the possible methods for generating laser  $TEM_{01*}$  mode with radial polarization includes two steps. A laser with a conical total mirror in its resonator will generate azimuthally polarized output radiation. It can be transformed to radial with two  $\lambda/2$  retarders.

## 5. REFERENCES

1. F.O.Olsen "Studies of Sheet Metal Cutting with Plane-Polarized CO<sub>2</sub>-laser". Proc. 5<sup>th</sup> annual Congress of Opto Electronics in Engineering (Laser-81) Munich, p.227-231, 1982.
2. G.Simon and U. Gratzke, "Theoretical Investigations of Instabilities in Laser Gas Cutting," SPIE, Vol.1132, pp. 204-209, 1989
3. A.V. La Rocca, L. Rorsati and M. Cantello, "Nozzle Design to Fluid Dynamics Effects in Laser Cutting," SPIE, Vol. 2207, pp. 48-62, 1994.
4. D.Schuocker, "Theoretical Model of Reactive Gas Assisted Laser Cutting Including Dynamic Effects" J. Appl. Phys. B, Vol. 40, pp. 9-14, 1986.
5. M. Vicanek and G.Simon, "Momentum and Heat Transfer of an Inert Gas Jet to the Melt in Laser Cutting," J.Phys. D: Appl Phys, Vol. 20, pp. 1191-1196, 1987.
6. A.F.H. Kaplan, "An Analytical Model of Metal Cutting, " J.Appl.Phys., **79** (5), pp. 2198-2199, 1996.
7. A.F.H. Kaplan, O. Wangler and D. Schuocker, "Laser Cutting: Fundamentals of the Periodic Striations and Their on-Line Direction," Lasers in Engineering, Vol. **2**, pp. 103-126, 1997.
8. W. Schulz, G. Simon, H.M. Urbassek and I. Decker, "On Laser Fusion Cutting," J.Phys. D: Appl. Phys., Vol. 20, pp. 481-488, 1986.
9. G.P. Cherepanov and A.G.Cherepanov, "Shape and Depth at Laser Beam Cutting", Physics and Chemistry of Material Processing (in Russian), Vol. 2, pp. 133-137, 1990.
10. D. Petring, P. Abels and E.Beyer, "Absorption Distribution on Idealized Cutting Front Geometries and its Significance for Laser Beam Cutting," SPIE, Vol.1020, pp. 123-131, 1988.
11. V.G.Niziev, "Theory of CW Laser Beam Cutting," Laser Physics, Vol. 3, '3, pp. 629-635, 1993.
12. J-M. Weick and W.Bartel, "Laser Cutting without Oxygen and its Benefits for Cutting Stainless Steel," Proc. 6<sup>th</sup> Int. Conf. Lasers in Manufacturing, pp. 81-89, May 1989.
13. E.Beyer, K.Wissenbach, G.Herzinger *Feinwerktechnik und Messtechnik* 1984, **92**, 3, S.141-143.
14. N.N. Rykalin, A.A. Uglov, I.V. Zuev and A.N. Kokora, "Laser Material Processing" (in Russian) Moscow, Mashinostroenie, , 496 p, 1985.
15. A.A. Vedenov, O.P. Ivanov and A.L. Chernyakov, "Theory of Destruction of Opaque Material Surface by Laser Radiation," Sov. J. Quant. Electron., Vol. 14, pp. 1587-91, 1984
16. W. Schulz, G. Simon and M.Vicanek, "Ablation of Opaque Surfaces due to Laser Irradiation, " J. Phys. D: Appl. Phys., Vol. 19, pp. 173-177, 1986
17. R. Nuss and S.Biermann, "Auswirkung der Polarisierung beim Laserstrahlschneiden," *Laser und Optoelektronik*, Vol. 4, pp. 389-392, 1987.
18. Handbook of Lasers with Selected Data on Optical Technology. Edited by R.J. Pressley. Chemical Rubber Co, Cleveland, 1971.
19. J. Powell, "CO<sub>2</sub> - Laser Cutting", Springer Verlag, 1993, p.16.